Time Domain Random Walks for Hydrodynamic Transport in Heterogeneous Media

Anna Russian[1], Marco Dentz[2], Philippe Gouze[1]

Abstract. We derive a general formulation of the time domain random walk (TDRW) approach to model the hydrodynamic transport of inert solutes in complex geometries and heterogeneous media. We demonstrate its formal equivalence with the discretized advection-dispersion equation and show that the TDRW is equivalent to a continuous time random walk (CTRW) characterized by space-dependent transition times and transition probabilities. The transition times are exponentially distributed. We discuss the implementation of different concentration boundary conditions and initial conditions as well as the occurrence of numerical dispersion. Furthermore, we propose an extension of the TDRW scheme to account for mobile-immobile multirate mass transfer. Finally, the proposed TDRW scheme is validated by comparison to analytical solutions for spatially homogeneous and heterogeneous transport scenarios.

1. Introduction

Hydrodynamic transport in heterogeneous media is a ubiquitous process in natural and engineered environments ranging from solute transport in geological media to the transport of charge carriers in amorphous semiconductors. Spatial inhomogeneity of the media and resulting flow fluctuations prohibit closed form analytical solutions for the distribution of the transported quantities. Here we focus on numerical random walk particle tracking methods for the solution of advective-dispersive transport in heterogeneous flow fields. In this framework the solute concentration is represented by the density distribution of non-interacting point-like solute particles which move due to advection and dispersion. Classical random walk particle schemes [*Kinzelbach*, 1987; *Salamon et al.*, 2006] rely on the strict equivalence between the Langevin equation, which describes the movement of non-interacting point particles due to advection and an uncorrelated random velocity (noise), and the advection-dispersion equation. Note that the independence of single particles make random walk methods intrinsically adapted to massively parallel computations, which often represents a noticeable advantage in terms of computation time. Classical random walk particle tracking methods discretize the Langevin equation in time so that particle motion occurs at discrete time steps with variable spatial increment that depends on the local velocity given by the flow field and the random noise. This classical approach could be termed discrete time random walk.

Generalization of this approach moves particles by spatial steps of variable length during variable time increments or transition times. This approach is generally known as the continuous time random walk (CTRW) [e.g., *Metzler and Klafter*, 2000; *Berkowitz et al.*, 2006]. The particle density, or equivalently the solute distribution, obeys a generalized Master equation [*Kenkre et al.*, 1973] and, when localizable in space, a generalized advection-dispersion equation [*Berkowitz et al.*, 2002; *Dentz and Berkowitz*, 2003]. The continuous time random walk (CTRW) has been used to upscale and model anomalous transport behaviors in heterogeneous media at pore, Darcy and regional scales [e.g., *Berkowitz and Scher*, 1997; *Berkowitz et al.*, 2006; *Le Borgne et al.*, 2008; *Dentz and Castro*, 2009; *De Anna et al.*, 2013; *Edery et al.*, 2014]). The heterogeneous medium or flow properties are mapped onto the coupled distribution of transition length and time which renders an ensemble average transport picture.

We focus on the modeling of hydrodynamic transport in deterministic media and flow fields with a well defined spatial variability, which can be given by the mapping of the pore structure or the porosity distribution extracted from X-ray microtomography images [*Gjetvaj et al.*, 2015; *Gouze et al.*, 2008] or computed from spatially variable hydraulic conductivity fields or fracture network geometries. Classical random walk particle tracking methods may induce high computational costs in media that display a broad range of velocity values because particles may spend a large number of random walk steps in low velocity areas due to the constant time discretization. The efficiency of particle tracking can be noticeably enhanced by moving a particle over a fixed distance imposed by the computational mesh, for example, in a time that corresponds to the transit time over this distance [e.g., *Pollock*, 1988; *McCarthy*, 1993; *Banton et al.*, 1997; *Noetinger and Estebenet*, 2000]. Variants of this general methodology have been known in the literature under the terms time domain random walk (TDRW) [*Banton et al.*, 1997; *Delay et al.*, 2002; *Cvetkovic et al.*, 2014; *Bodin*, 2015] and CTRW [*McCarthy*, 1993; *Noetinger and Estebenet*, 2000]. As a general concept, the TDRW moves particles on a lattice with jumps of fixed distance whose direction and transition times are determined by the local advection and dispersion (or diffusion). However, we have found that there is a certain ambiguity in the modeling of the distribution of local time increments. For instance *McCarthy* [1993]; *Noetinger and Estebenet* [2000], and *Delay et al.* [2002] used exponential transition time distributions, whose mean is given by the local advection dispersion properties, *James and Chrysikolpoulos* [2001] and *Delay and Bodin* [2001] propose to use a log-normal transition time distribution, while *Reimus and James* [2002] associated the local transition time to the first passage time to cross the transition distance by diffusion. *Dentz et al.* [2012] have shown for heterogeneous diffusion problems, the equivalence between the TDRW and the diffusion equation requires an exponential distribution of local transition times. This is an

[1]Géoscience, Université de Montpellier 2, CNRS, Montpellier, France.
[2]Institute of Environmental Assessment and Water Research (IDAEA), Spanish National Research Council (CSIC), Barcelona, Spain.

0043-1397 /16/$9.00

expression of local memorylessness because the local transport details are fully resolved. Furthermore, it has been pointed out in the literature [*Delay et al.*, 2002; *Dentz et al.*, 2012] that the TDRW is equivalent to discretized versions of the dispersion equation. Here we extend the work of *Dentz et al.* [2012] to the hydrodynamic transport. It is well-known that numerical methods that rely on discrete versions of the advection-dispersion equation suffer from numerical dispersion. Thus, the TDRW method, even though particle based, may suffer from similar effects. Notice that numerical dispersion in classical random walk methods is eliminated in the scale limit of infinitesimal constant transit times. Here the finite spatial discretization imprints also a dispersion scale. Thus, the issues of the choice of the local transit time distribution and of the presence of numerical dispersion must be addressed for reliable TDRW modeling of the hydrodynamic transport in heterogeneous media.

Section 2 establishes the formal equivalence between the discretized advection-dispersion equation and the TDRW scheme using the CTRW formalism. Then we extend the numerical scheme to model mobile-immobile multirate mass transfer (MRMT). Section 3 provides details on the numerical implementation of boundary condition in the TDRW and investigates the issue of numerical dispersion. Section 4 illustrates the accuracy of the proposed TDRW scheme by comparing the results with analytical solutions for different diffusion-advection scenarios in homogeneous and heterogeneous velocity fields and under multirate mass transfer.

2. Theoretical Development

The transport of a non-reactive solute at pore scale can be described by the advection-diffusion equation. At the Darcy scale, transport may be described by the advection-dispersion equation [*Bear*, 1972]. The validity of such (asymptotic) Fickian transport descriptions for solute transport in heterogeneous media at practically relevant spatial and temporal scales has been a debated issue [*Berkowitz et al.*, 2006; *Neuman and Tartakovsky*, 2009], but is not the scope to the present paper. However, we will show in Section 2.2 that the TDRW approach can be extended for the modeling of non-Fickian transport. We consider the general advection-dispersion equation for passive transport in a heterogeneous medium, which is characterized by spatial variability in the transport velocity $\mathbf{v}(\mathbf{x})$ and the dispersion coefficient $D(\mathbf{x})$. It is given by

$$\frac{\partial c(\mathbf{x},\mathbf{t})}{\partial t} + \nabla \cdot [\mathbf{v}(\mathbf{x})\mathbf{c}(\mathbf{x},\mathbf{t})] - \nabla \cdot \mathbf{D}(\mathbf{x})\nabla \mathbf{c}(\mathbf{x},\mathbf{t}) = \mathbf{0} \quad (1)$$

with suitable initial and boundary conditions.

2.1. Derivation of the Time-Domain Random Walk

The derivation of the advective TDRW scheme starts from the finite volume discretization of (1), which can be written as [*Delay et al.*, 2002]

$$V_i \frac{\partial c_i(t)}{\partial t} = \sum_{[ij]} b_{ij} V_j c_j(t) - \sum_{[ij]} b_{ji} V_i c_i(t), \quad (2)$$

where $c_i(t)$ is the concentration at voxel i. The notation $\sum_{[ij]}$ indicates the summation over the nearest neighbors of voxel i and b_{ij} defined as

$$b_{ij} = \frac{S_{ij}\hat{D}_{ij}}{V_j|\xi_{ij}|} + \frac{S_{ij}|v_{ij}|}{2V_j}\left(\frac{v_{ij}}{|v_{ij}|}+1\right), \quad (3)$$

where S_{ij} denotes the surface area between voxels i and j and V_j denotes the volume of voxel j. The vector $\boldsymbol{\xi}_{ij}$ points from voxel j to voxel i; its absolute value is denoted by $|\xi_{ij}|$. Accordingly, the velocity component v_{ij} of $\mathbf{v}_j$ denotes the velocity at voxel j in direction of voxel i and is equal to $\mathbf{v}_j \cdot \boldsymbol{\xi}_{ij}/|\xi_{ij}|$. If $v_{ij} > 0$, voxel i is downstream from voxel j, and correspondingly, if $v_{ij} < 0$ voxel i is upstream from voxel j. Note that here $b_{ij} \neq b_{ji}$ whereas $b_{ij} = b_{ji}$ for the pure-diffusion problem. $\hat{D}_{ij}$ is the effective diffusion coefficient between voxel i and voxel j. In a $d = 1$ dimensional medium the inter-voxel diffusion coefficient $\hat{D}_{ij}$ is given by the harmonic mean while the geometric mean is required for $d = 2$ [*Noetinger and Estebenet*, 2000; *Dentz et al.*, 2012]. For the general case ($d = 3$) the inter-voxel diffusion coefficient $\hat{D}_{ij}$ is not constrained by theoretical demonstrations so far.

In order to establish the particle based numerical TDRW scheme, we formulate (2) as a Master equation. To this end, we first define the density $g_i(t)$ of particles at node i as

$$g_i(t) = V_i c_i(t). \quad (4)$$

We furthermore define the transition probabilities w_{ij} from node j to node i and the time τ_j for the transition of a particle from node j to one of the next neighbor nodes as

$$w_{ij} = \frac{b_{ij}}{\sum_{[jk]} b_{kj}} \qquad \tau_j = \frac{1}{\sum_{[jk]} b_{kj}}. \quad (5)$$

Note that, in general, the transition probabilities are not symmetric, $w_{ij} \neq w_{ji}$. By definition they fulfill the normalization condition $\sum_{[ji]} w_{ij} = 1$. With these definitions, we identify (2) with the Master equation [*Kenkre et al.*, 1973]:

$$\frac{dg_i(t)}{dt} = \sum_{[ij]} w_{ij}\tau_j^{-1} g_j(t) - \tau_i^{-1} g_i(t). \quad (6)$$

This Master equation describes the evolution of the particle density $g_i(t)$ in the following lattice random walk. The random walkers or particles move between the vertices of a lattice which are located at the center-point of the voxels (which accordingly form a meshed representation of the studied media). The particle move according to the following recursion relations:

$$\mathbf{x}_i(n+1) = \mathbf{x}_j(n) + \boldsymbol{\xi}_{ij}, \qquad t(n+1) = t(n) + \theta_j. \quad (7)$$

The probability for the spatial transition of the particle from the vertex at $\mathbf{x}_j$ to the neighboring vertex $\mathbf{x}_i = \mathbf{x}_j + \boldsymbol{\xi}_{ij}$ is given by the w_{ij} defined in (5). The transition times θ_j are distributed according to the exponential transition time PDF

$$\psi_j(t) = \frac{\exp(-t/\tau_j)}{\tau_j}, \quad (8)$$

where τ_j is given by (5).

In order to see this equivalence, we consider the inhomogeneous continuous time random walk (CTRW) defined by the recursion relation (7) and characterized by a general location-dependent transition time PDF $\psi_j(t)$. It has been shown [*Scher and Lax*, 1973; *Berkowitz et al.*, 2006; *Dentz et al.*, 2012] that the $g_i(t)$ satisfies the generalized Master equation [*Kenkre et al.*, 1973]

$$\frac{dg_i(t)}{dt} = \int_0^t dt' \sum_{[ij]} w_{ij} M_j(t-t') g_j(t') - \int_0^t dt' M_i(t-t') g_i(t'), \quad (9)$$

where the memory kernel is defined by its Laplace transform as

$$M_j^*(\lambda) = \frac{\lambda\psi_j^*(\lambda)}{1-\psi_j^*(\lambda)}. \tag{10}$$

The Laplace transform [*Abramowitz and Stegun*, 1972] is denoted here by an asterisk and the Laplace variable by λ. For the transition time distribution (8), the memory function reduces to

$$M_j(t) = \frac{1}{\tau_j}\delta(t). \tag{11}$$

Inserting this expression into (9) gives directly the Master equation (6) and thus shows the equivalence of the discrete advection-dispersion equation (2) and the TDRW scheme characterized by the recursion relations (7), the transition probabilities (5) and the transition time PDF (8).

2.2. Modeling of Multirate Mass Transfer

Here we briefly detail the generalization of the advective-dispersive TDRW scheme to account for multirate mass transfer (MRMT) [e.g., *Haggerty and Gorelick*, 1995; *Carrera et al.*, 1998]. The methodology follows closely the one described in *Dentz et al.* [2012]. The MRMT approach accounts for transport combined with retardation mechanisms due to particle or solute traps, or immobile zones. The immobilization mechanisms can be chemical, such as adsorption, and physical, such as diffusion into dead end pores, immobile microporosity, and slow advection in low permeability inclusions. The modeling of advective-dispersion transport through TDRW and its combination with MRMT is based on the works of *Dentz and Berkowitz* [2003] and *Benson and Meerschaert* [2009], who formulated the MRMT approach in the CTRW framework, and the work of *Margolin et al.* [2003], who establish a transition time PDF for the CTRW approach that accounts for multirate particle trapping.

In the TDRW (7) advective-dispersive particle transitions are reflected by the transition time θ_j, which is exponentially distributed according to (8). In the presence of particle traps, the transition time is given by the sum of the exponential transition time θ_j and the total time of the trapping events that occur during an advective-dispersive transition. Thus, the total transition time Θ_j is given by

$$\Theta_j = \theta_j + \sum_{l=1}^{n_{\theta_j}} \vartheta_{jl}, \tag{12}$$

with the trapping times ϑ_{jl}, which are distributed according to $p_j(t)$. The trapping process occurs at constant rate α_j during the advective-dispersive transition such that the number of trapping events n_{θ_j} is a Poisson-distributed random variable. Thus, the total transition time PDF $\Psi(t)$ describes a compound Poisson process. Its PDF $\psi(t)$ can be expressed in Laplace space as [*Margolin et al.*, 2003; *Dentz et al.*, 2012]

$$\psi_j^*(\lambda) = \frac{1}{1+\lambda\tau_j+\alpha_j\tau_j[1-p_j^*(\lambda)]}. \tag{13}$$

Inserting (13) into the Laplace transform of the generalized Master equation (9) and using the definition (5) of the transition probabilities w_{ij} and the characteristic transition time τ_j, we obtain

$$\lambda V_i c_i^*(\lambda) = \rho_i + \sum_{[ij]} b_{ij}\frac{\lambda V_j c_j^*(\lambda)}{\lambda+\alpha_j[1-p_j^*(\lambda)]} - \sum_{[ij]} b_{ji}\frac{\lambda V_i c_i^*(\lambda)}{\lambda+\alpha_i[1-p_i^*(\lambda)]}, \tag{14}$$

where ρ_i denotes the initial concentration distribution. Note that we used (4) to substitute the number density $g_i^*(\lambda)$ by the concentration $c_i^*(\lambda)$. We define now the mobile concentration $c_{i,m}(t)$ through the Laplace transform

$$c_{i,m}^*(\lambda) = \frac{\lambda c_i^*(\lambda)}{\lambda+\alpha_i[1-p_i^*(\lambda)]}, \tag{15}$$

and the trapped concentration $c_{i,t}(t)$ through

$$c_{i,t}^*(\lambda) = c_i^*(\lambda) - c_{i,m}^*(\lambda) = \varphi_i^*(\lambda)c_{i,m}^*(\lambda), \tag{16}$$

with the transfer function defined as:

$$\varphi_i^*(\lambda) = \alpha_i[1-p_i^*(\lambda)]. \tag{17}$$

Using these definitions in (14) and performing the inverse Laplace transform gives

$$\frac{dV_i c_{i,m}(t)}{dt} + \frac{d}{dt}\int_0^t dt'\varphi(t-t')V_i c_{i,m}(t-t') = \sum_{[ij]} b_{ij}V_j c_{j,m}(t) - \sum_{[ij]} b_{ji}V_i c_{i,m}(t). \tag{18}$$

In the spatial continuum limit, this equation becomes

$$\frac{\partial c_m(\mathbf{x},t)}{dt} + \frac{\partial}{\partial t}\int_0^t dt'\varphi(\mathbf{x},t-t')c_m(\mathbf{x},t-t') = -\nabla\cdot\mathbf{v}(\mathbf{x})c_m(\mathbf{x},t) + \nabla\cdot\mathbf{D}(\mathbf{x})\nabla c_m(\mathbf{x},t). \tag{19}$$

with the transfer function

$$\varphi^*(\mathbf{x},\lambda) = \frac{\alpha(\mathbf{x})}{\lambda}[1-p^*(\mathbf{x},\lambda)]. \tag{20}$$

3. Numerical Implementation

Here we detail the numerical implementation of the proposed TDRW scheme for modeling hydrodynamic transport. In a discretized domain particle position is updated according to (7) with the transition probabilities w_{ij} given in (5). The transition time is drawn for each particle from the exponential distribution (8) with mean transition time τ_j given by (5). Thus, time increment may be re-written as

$$t_{n+1} = t_n + \theta_j, \qquad \theta_j = -\tau_j\ln(\eta_n), \tag{21}$$

where θ_j is the random time increment and η_n is a random variable uniformly distributed in $(0,1]$. In the following, we discuss the implementation of boundary conditions. We study the occurrence of numerical dispersion in the advective dispersive TDRW scheme and finally report in the implementation of MRMT.

3.1. Boundary Conditions

For simplicity, we discuss the boundary conditions for $d = 1$ dimensional scenarios. The generalization to d dimensions is straightforward.

3.1.1. Concentration Boundary Condition

An instantaneous constant concentration boundary is defined by

$$c(x=0,t) = k_0\delta(t), \tag{22}$$

where k_0 is an injection rate. The boundary of the domain is located between the 2nd and 3rd voxels of the computational mesh, which have the size $|\xi|$. We assign to the 1st, 2nd and 3rd voxels the same values for the diffusion coefficients, D_0, and the velocities, v_0. Then N_p particles are place in the 2nd voxel. At the first jump each particle moves according to the corresponding transition probabilities. The particles that transition to the 1st voxel are removed from the system. At subsequent jumps, particles that arrive at the 2nd voxel are removed, which simulates the absorbing boundary condition for times $t > 0$. With this implementation, the numerical boundary concentration $\hat{c}(x=0,t)$, i.e., the concentration in the boundary voxel is actually given by

$$\hat{c}(x=0,t) = \frac{\exp(-t/\tau_b)}{\xi} \tag{23}$$

because the residence time is exponentially distributed. The characteristic residence τ_b in the boundary voxel is given by

$$\tau_b = \frac{\tau_{v_0}}{1+2\epsilon_0}, \tag{24}$$

where $\tau_{v_0} = |\xi|/v_0$ and $\epsilon_0 = D_0/(v_0|\xi|)$. We can rewrite (23) as

$$\hat{c}(x=0,t) = \frac{\tau_b}{\xi}\frac{\exp(-t/\tau_b)}{\tau_b} \approx \frac{\tau_b}{\xi}\delta(t). \tag{25}$$

in the limit of τ_b much smaller than the observation time. Thus, the desired concentration $c(x,t)$ with the boundary condition (22) is given by

$$c(x,t) = \frac{k_0\xi}{\tau_b}\hat{c}(x,t) \tag{26}$$

Note that $\tau_b/\xi = v_0^{-1}/(1+2\epsilon_0)$, and in the absence of diffusion at the boundary, that is $D_0 = 0$, we simply have that $\tau_b/\xi = v_0^{-1}$.

For a finite concentration pulse at the boundary, i.e., for

$$c(x=0,t) = c_b(t) \tag{27}$$

the concentration $c(x,t)$ can be expressed according to Duhamel's theorem in terms of the concentration $g(x,t)$ for the pulse boundary condition $g(x=0,t) = \delta(t)$ as

$$c(x,t) = \int_0^t dt' g(x,t-t')c_b(t'). \tag{28}$$

Thus, the solution $c(x,t)$ can be obtained by the solution for a pulse boundary condition through the convolution (28). The Green function $g(x,t)$ is obtained by setting $k_0 = 1$ in (22).

Alternatively, the solution $c(x,t)$ can be obtained by placing particles at random times $t' > 0$, which are distributed according to

$$\chi(t') = \frac{c_b(t')}{\int_0^\infty d\tau c_b(\tau)}. \tag{29}$$

Thus, the numerical concentration $\hat{c}(x=0,t)$ at the boundary then is given by

$$\hat{c}(x=0,t) = \int_0^\infty dt' \frac{\tau_b}{\xi} p_b(t') \frac{\exp[-(t-t')/\tau_b]}{\tau_b}. \tag{30}$$

Thus, the desired concentration $c(x,t)$ is obtained from the numerical concentration as

$$c(x,t) = \frac{\xi \int_0^\infty d\tau c_b(\tau)}{\tau_b}\hat{c}(x,t). \tag{31}$$

Note that for a finite-duration constant concentration initial condition (or for a constant continuous injection), the particle are placed at random time t' uniformly distributed between 0 and the end time of the injection time (or till the end time of the simulation in case of a continuous injection).

3.1.2. Flux Boundary Condition

An instantaneous flux boundary condition is expressed as

$$j_0(t) = \left[vc(x,t) - D\frac{\partial c(x,t)}{\partial x}\right]_{x=0} = \delta(t). \tag{32}$$

This boundary condition is simulated numerically by placing particles at time $t = 0$ at the second voxel of the computational domain. The boundary is located between the 1st and 2nd voxels. The diffusion coefficient and velocity in the 1st voxel are 0, in the 2nd voxel they are given by D_0 and v_0. Thus, the numerical flux $\hat{j}_0(t)$, i.e., the distribution of times needed to cross the boundary voxel is simply given by the residence time distribution

$$\hat{j}_0(t) = \frac{\exp(-t/\tau_b)}{\tau_b}. \tag{33}$$

In the limit of τ_b much smaller than the observation time, it approximates well the boundary condition (32).

In order to model a continuous injection at the boundary,

$$j_0(t) = j_b(t) \tag{34}$$

we proceed in the same way as for the concentration boundary in the previous section. We note that the concentration $c(x,t)$ is given by Duhamel's theorem in terms of the Green function $g(x,t)$, which satisfies the boundary condition (32), as

$$c(x,t) = \int_0^t dt' g(x,t-t')j_b(t'). \tag{35}$$

Thus, $c(x,t)$ can be simply obtained by convolution of the solution of the instantaneous flux boundary condition.

Alternatively, it can be obtained, as above, by injection of particles at random times t' distributed according to

$$\chi(t') = \frac{j_b(t')}{\int_0^\infty d\tau j_b(\tau)}. \tag{36}$$

Thus, the numerical flux $\hat{j}_0(t)$ at the boundary then is given by

$$\hat{j}_0(t) = \int_0^\infty dt' \chi(t') \frac{\exp[-(t-t')/\tau_b]}{\tau_b} \tag{37}$$

and the desired concentration $c(x,t)$ is obtained from the numerical concentration $\hat{c}(x,t)$ as

$$c(x,t) = \left[\int_0^\infty d\tau c_b(\tau)\right] \hat{c}(x,t). \tag{38}$$

3.2. Numerical Dispersion

The TDRW is based on a finite volume discretization of the advection-dispersion equation. Thus, even though it represents a particle scheme, it is susceptible to numerical dispersion. This is owed to the fact that the TDRW is based on a lattice random walk. Here, we derive a criterion the estimation of the numerical dispersion. For simplicity, we present the derivation here for $d = 1$ dimension and a constant dispersion coefficient. We start from the Master equation (6) for $d = 1$, which we write as

$$\begin{aligned}\frac{dc(x_i,t)}{dt} = &\frac{D(x-\xi)}{\xi^2}c(x_i-\xi,t) + \frac{D(x_i+\xi)}{\xi^2}c(x_i+\xi,t)\\ &- \frac{D(x_i-\xi)+D(x_i+\xi)}{\xi^2}c(x_i,t)\\ &+ \frac{v(x_i-\xi)c(x_i-\xi) - v(x_i)c(x_i,t)}{\xi},\end{aligned} \tag{39}$$

We substitute here $v_j \to v(x_i-\xi)$, $\hat{D}_{ii-1} \to D(x_i-\xi)$ and $\hat{D}_{ii+1}$ accordingly. In the limit of $\xi \to 0$, we obtain by expanding up to order ξ

$$\begin{aligned}\frac{\partial c(x,t)}{\partial t} = &-\frac{\partial}{\partial x}\left[v(x) - \frac{\xi}{2}\frac{dv(x)}{dx}\right]c(x,t)\\ &+ \frac{\partial}{\partial x}\left[D(x) + \frac{v(x)\xi(x)}{2}\right]\frac{\partial c(x,t)}{\partial x} + \ldots,\end{aligned} \tag{40}$$

where the dots denote contributions of order ξ^2. Thus, the TDRW scheme exhibits numerical dispersion as well as an artificial drift that is proportional to the derivative of the flow velocity $v(x)$. As the flow fields under consideration are typically smooth, the latter effect can be disregarded. In order to suppress the impact of numerical dispersion, the coefficient $v(x)|\xi|/2$ should be smaller than the actual dispersion coefficient $D(x)$, the discretization ξ should be chosen such that the condition

$$|\xi| < \frac{2D(x)}{|v(x)|} \tag{41}$$

is fulfilled.

3.3. Implementation of Multirate Mass Transfer

As explained in Section 2.2, a particle can get trapped a number n_j of times during its transition time θ_j and remain trapped during a time ϑ_{jl}. Therefore the total transition time is given by the *mobile* transition time θ_j plus the sum over the trapping times ϑ_{jl} given in (12). Thus the particle time is updated as

$$t_{n+1} = t_n + \theta_j + \sum_{l=1}^{n_{\theta_j}} \vartheta_{jl}. \tag{42}$$

As outlined in Section 2.2, trapping events occur at a constant rate α_j during a particle transition characterized by a mobile time θ_j, which is given by (21). Thus, the number of trapping event n_{θ_j} drawn from the Poisson distribution

$$\nu(n|\theta_j) = \frac{(\alpha_j\theta_j)^n}{n!}\exp(-\alpha_j\theta_j). \tag{43}$$

The trapping times ϑ_{jl} are drawn from the distribution $p_j(t)$.

4. Validation

In this section, we validate the proposed TDRW approach for a series of homogeneous and inhomogeneous advection-dispersion scenarios under multirate mass transfer.

4.1. Homogeneous Semi-Infinite Domain

As the simplest case, we consider a $d = 1$ homogeneous domain, where ADE equation reads:

$$\frac{\partial c(x,t)}{\partial t} + v\frac{\partial c(x,t)}{\partial x} - D\frac{\partial^2 c(x,t)}{\partial x^2} = 0 \tag{44}$$

with diffusivity D and velocity v homogeneous and constant. For the first example we record the temporal evolution of the resident concentration at given distances from the inlet where the condition is a constant resident concentration. For the second example the inlet boundary condition is a constant flux and we record both the temporal evolution of the resident concentration and the first arrival time at given distances from the inlet.

4.1.1. Dirichlet Boundary Condition: Instantaneous Injection

Firstly we take into account temporal evolution of concentration in a semi-infinite domain with instantaneous constant concentration at the inlet:

$$\begin{aligned} c(0,t) &= j_0\delta(t) \\ c(x,0) &= 0 \qquad\qquad x > 0 \\ \lim_{x\to\infty} c(x,t) &= 0 \end{aligned} \tag{45}$$

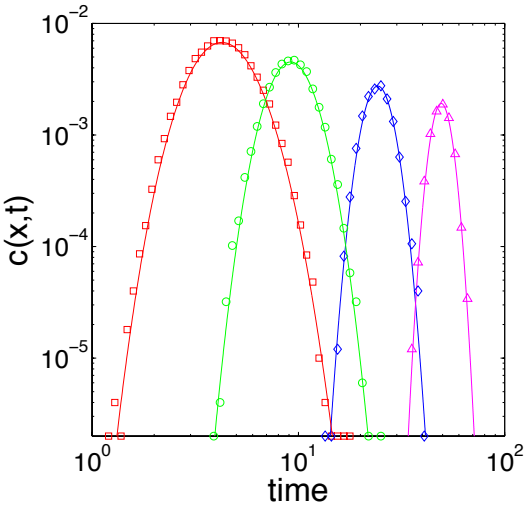

Figure 1. Temporal evolution of residence concentration observed at different observation points for a semi-infinite $d = 1$ dimensional domain with constant concentration BC at the inlet. Lines: analytical solution given in (46), symbols: TDRW simulations. Parameters (all values are expressed in consistent arbitrary length and time units): $D = 1$, $v = 2$, observation points: $x = 10$ (squares), $x = 20$ (circles), $x = 50$ (rhombus) and $x = 100$ (triangles). Parameters for the TDRW simulations: number of particles $N_p = 10^7$, voxel size: $\xi = 0.05$.

The analytical solution of (44) with conditions (45) was given by *Kreft and Zuber* [1978]:

$$c(x,t) = j_0 \frac{x}{\sqrt{4\pi D t^3}} \exp\left[-\frac{(x-vt)^2}{4Dt}\right]. \qquad (46)$$

Numerically, the boundary conditions 45 are approximated as explained in Section 3.1. Thus, the constant j_0 is equal to τ_b/ξ with τ_b the residence time of the initial boundary voxel.

In the particle tracking framework the normalized concentration is given by the number of particles arriving at the observation voxel, n_p, divided by the total number of particles of the simulation N_p and by the voxel size ξ, thus: $c^p(x,t) = n_p/N_p/\xi$. Figure 1 successfully compares the results of the numerical simulations with the analytical solution. Parameter of the simulations are given in the caption of the figure.

Notice that the problem of computing the temporal evolution of resident concentration with boundarires conditions (45) is equivalent to the problem of injection in flux and detection in flux, or rather in the computation of the first passage time distribution for an istantaneous flux injection [*Kreft and Zuber*, 1978].

4.1.2. Dirichlet Boundary Condition: Continuous Injection

Here we considered a fixed constant concentration as inlet boundary condition

$$c(0,t) = c_0 \qquad (47)$$
$$\lim_{x\to\infty} c(x,t) = 0.$$

and we compute the cumulative concentration at a given observation point. As mentioned before, notice that this problem is equivalent to compute the first passage time distribution for a continuous flux injection at the inlet boundary.

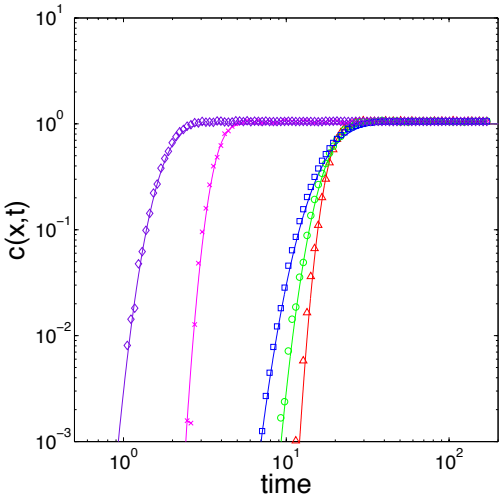

Figure 3. Temporal evolution of the cumulative concentration for different values of velocities and diffusivity. Lines indicate the computed inverse Laplace transform of the analytical solution given in Eq.(48). Symbols are result of the TDRW simulations: (squares) $D = 1$, $v = 1$, (circles) $D = 0.5$, $v = 1$, (triangles) $D = 0.2$, $v = 1$, (crosses) $D = 1$, $v = 5$, (rhombus) $D = 5$, $v = 10$. Parameters: $d = 1$ dimensional domain; domain size $L = 250$, observation points: $x = 20$, number of particles $N_p = 10^6$, voxel size $\xi = 0.1$. All values are expressed in consistent arbitrary length and time units.

The numerical procedure for computing the first passage time distribution using TDRW consists simply in removing the particles that reach the observation point. The analytical solution is given by *Kreft and Zuber* [1978]:

$$c(x,t) = \frac{1}{2}\,\mathrm{erfc}\left(\frac{x-vt}{\sqrt{4Dt}}\right) + \frac{1}{2}\exp\left(\frac{vx}{D}\right)\mathrm{erfc}\left(\frac{x+vt}{\sqrt{4Dt}}\right) \qquad (48)$$

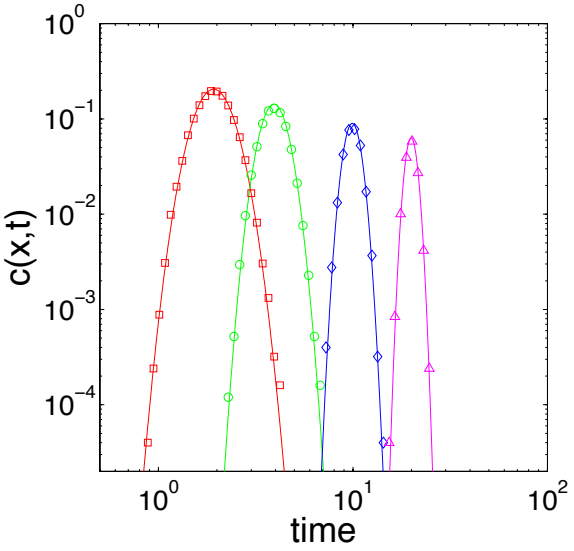

Figure 4. Temporal evolution of the resident concentration observed at different observation points in a semi-infinitive $d = 1$ dimensional domain. Lines: analytical solution given in (50), symbols: TDRW simulations. Parameters (all values are expressed in consistent arbitrary length and time units): $D = 1$, $v = 5$, observation points: $x = 10$ (squares), $x = 20$ (circles), $x = 50$ (rhombus) and $x = 100$ (triangles). Parameters TDRW simulations: number of particles $N_p = 10^6$, voxel size: $\xi = 0.05$.

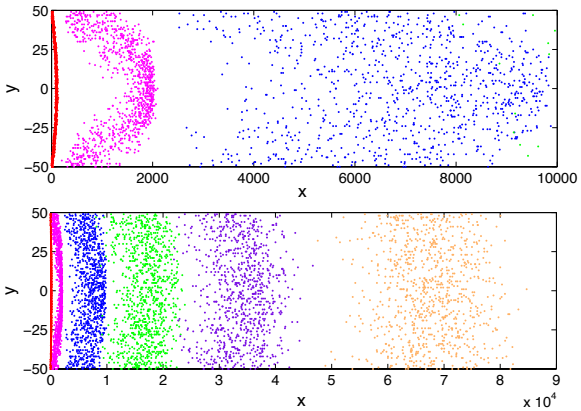

Figure 5. Distribution of solute particles evolving from a line source in a $d = 2$ dimensional domain with Newtonian velocity profile and line Figure top: from left to right distribution of particles for times t=10, 200 and 1000. Figure down: from left to right distribution of particles for times t=10, 200, 1000, 2500, 5000 and 10000, or rather for time $t = 10^{-3}\tau_D$, $t = 2\cdot 10^{-2}\tau_D$, $t = 0.1\tau_D$, $t = 0.25\tau_D$, $t = 0.5\tau_D$ and $t = \tau_D$. Parameters: $D = 1$, $v_m = 10$, $\ell_y = 100$. All values are expressed in consistent arbitrary length and time units.

Figure 3 displays the successful comparison between the TDRW simulations and the analytical solution (48) for different values of (spatially constant) diffusivity and velocity (parameters are given in the caption of the figure).

4.1.3. Robin Boundary Condition: Instantaneous Injection

Here we consider Eq. (44) with the following boundary conditions:

$$\left[v\,c(x,t) - D\frac{\partial c(x,t)}{\partial x}\right]_{x=0} = \delta(t), \qquad \lim_{x\to\infty} c(x,t) = 0 \tag{49}$$

The solution of (44) for a semi-infinite domain expressed in term of resident concentration was given by *Kreft and Zuber* [1978]:

$$c(x,t) = \frac{2}{\sqrt{4\pi D t}}\exp\left[-\frac{(x-vt)^2}{4Dt}\right] - \frac{v}{2D}\exp\left(\frac{vx}{D}\right)\operatorname{erfc}\left(\frac{x+vt}{\sqrt{4Dt}}\right) \tag{50}$$

Figure 4 shows that TDRW numerical simulations coincide with the analytical solution (50). The simulation parameters are given in the caption of the figure.

In order to test the algorithm for any d dimension, we performed TDRW for $d = 2$ and $d = 3$ dimension computing temporal evolution of concentration of a observation line and observation plane, respectively. Numerical simulations fully overlap the $d = 1$ simulations and consequently the $d = 1$ analytical solutions.

4.2. Newtonian Velocity Profile: Taylor dispersion

In the following we consider a $d = 2$ dimensional medium $\mathbf{x} = (x, y)$ and we use a Newtonian velocity profile along the y direction given by:

$$v(y) = v_m\left[1 - \frac{\left(y - \frac{\ell_y}{2}\right)^2}{\left(\frac{\ell_y}{2}\right)^2}\right] \tag{51}$$

where v_m is the maximum velocity reached in the middle of the domain and ℓ_y is the vertical dimension of the domain.

Figure 5 illustrates the distribution of the random walkers (or particles) issuing from a line source at different observation times. We take a semi-infinite domain with reflecting inlet boundary.

As observable quantity we considered the second centered moment $\kappa_x(t)$ given by the difference of the second and the first squared moment of the concentration along the x direction:

$$\kappa_x(t) = \langle x^2(t)\rangle - \langle x(t)\rangle^2, \tag{52}$$

where the squared brackets indicate the ensemble average over all the particles of the simulation. Figure 2 shows the second centered moment computed for different values of diffusivity in a $d = 2$ dimensional domain with a Newtonian velocity profile.

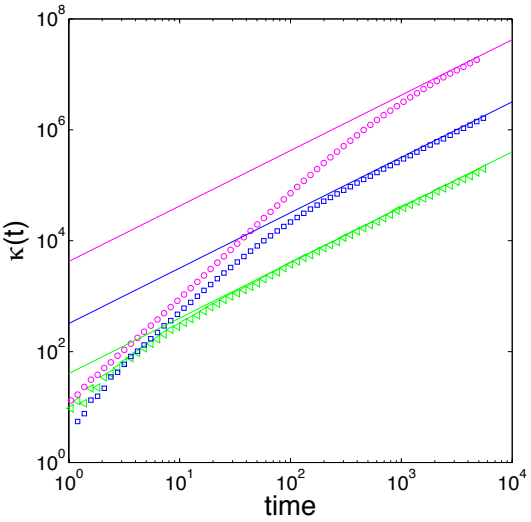

Figure 2. Temporal evolution of the mean squared displacement for a $d = 2$ dimensional domain considering a Newtonian velocity profile. Parameters (all values are expressed in consistent arbitrary length and time units): $v_m = 10$ $\ell_y = 100$, $D = 1$ (circles), $v_m = 10$ $\ell_y = 10$, $D = 1$ (triangles) and $D = 0.1$ (squares). Straight lines indicate the second centered moment for Taylor dispersion given by Eq. 53.

As it is shown in Figure 2 $\kappa(t)$ increases following a ballistic regime for $t < \tau_D$ with $\tau_D = \ell_y^2/D$ the mean diffusion time over the vertical direction and for $t > \tau_D$ $\kappa(t)$ increases linearly with time following the effective Taylor dispersion:

$$\kappa(t) = 2D\left(1 + \frac{1}{210}\frac{\overline{v}^2\ell_y^2}{D^2}\right)t, \tag{53}$$

where $\overline{v}$ is the average velocity $\overline{v} = 2v_m/3$.

4.3. Linear Shear Flow

Here we consider a $d = 2$ dimensional linear shear flow in an unbounded domain. The x axis of the coordinate system is aligned with the flow direction and y axis is perpendicular to x. The flow velocity is composed of a pure shear contribution αy, in which σ is the shear rate. Transport is given by:

$$\frac{\partial c(\mathbf{x},t)}{\partial t} + \sigma y\frac{\partial c(\mathbf{x},t)}{\partial x} - \nabla\cdot\mathbf{D}\nabla\mathbf{c}(\mathbf{x},\mathbf{t}) = \mathbf{0}. \tag{54}$$

We assume dispersion spatially uniform and isotropic thus the dispersion tensor is $D_{ij} = D$. The solution of (54) for a pulse injection is given by *Bolster et al.* [2011]:

$$c(\mathbf{x},t) = \frac{1}{2\pi\sqrt{||\boldsymbol{\kappa}(t)||}}\exp\left[-\frac{\mathbf{x}^T\boldsymbol{\kappa}^{-1}(t)\mathbf{x}}{2}\right] \tag{55}$$

with $||\boldsymbol{\kappa}(t)||$ the determinant of the variance matrix $\kappa(t)$:

$$\kappa_{11}(t) = 2Dt + \frac{2}{3}D\sigma^2t^3 \qquad \kappa_{12}(t) = D\sigma t^2 \tag{56}$$

$$\kappa_{21}(t) = D\sigma t^2 \qquad \kappa_{22}(t) = 2Dt \tag{57}$$

As observable quantity we choose the temporal evolution of the concentration arriving at a given observation plane perpendicular to the flow direction x. By integrating equation (55) along the y direction we obtain:

$$= \frac{1}{\sqrt{2\pi\kappa_{11}}} \exp\left[\frac{x_0^2}{2||\boldsymbol{\kappa}(t)||}\left(\frac{\kappa_{12}^2}{\kappa_{11}} - \kappa_{22}\right)\right] \qquad (58)$$

Figure 6 shows the temporal evolution of the integrated concentration at different distances. Results of TDRW simulations coincide with analytical solution (58).

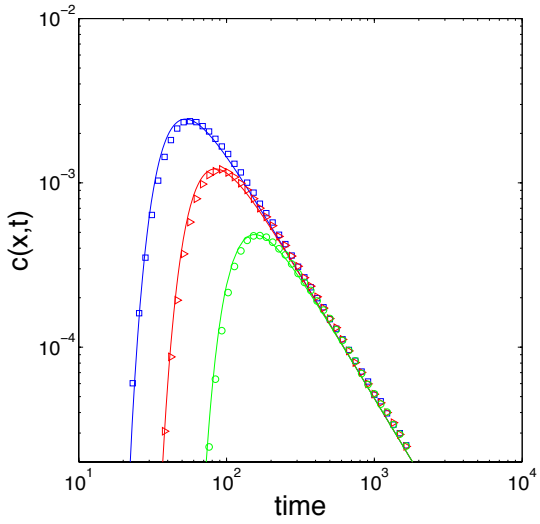

Figure 6. Temporal evolution of concentration at given observation planes for a linear shear flow. Parameters (all values are expressed in consistent arbitrary length and time units): $D = 0.1$, $\sigma = 1$, $x_1 = 100$ (squares), $x_2 = 200$ (triangles) and $x_3 = 500$ (circles).

4.4. Multirate Mass Transfer

Here we illustrate the performance of the MRMT extension to the advective-dispersive TDRW. As explained previously, the number of trapping events n_{θ_j} at voxel j depends on the total mobile time θ_j and is drawn from a Poisson distribution (43). We consider spatially homogeneous mass transfer properties characterized by a constant the trapping rate α and a single trapping time distribution $p(\tau)$. The trapping times are drawn from the Pareto distribution:

$$p(\tau) = \frac{\beta}{\tau_c}\left(\frac{\tau}{\tau_c}\right)^{-1-\beta}. \qquad (59)$$

We set here $\tau_c = 10^{-1}$. In the frame of the multirate mass transfer model such as proposed by *Haggerty and Gorelick* [1995] and *Carrera et al.* [1998], this corresponds to a power-law memory function scaling as $t^{-\beta}$ and a late time concentration of the breakthrough curve scaling as $t^{-1-\beta}$, for $t \gg \tau_c$.

We consider here an instantaneous injection into the flux at the inlet boundary at $x = 0$ of a semi-infinite domain such that

$$j(x = 0, t) = \delta(t), \qquad j(x = \infty, t) = 0. \qquad (60)$$

Thus, the solution for $j(x, t)$ can be obtained straightforwardly in Laplace space as

$$j^*(x, \lambda) = \exp\left[-\frac{vx}{2D}\left(\sqrt{1 + \frac{4D}{v^2}\lambda[1 + \varphi^*(\lambda)]} - 1\right)\right], \qquad (61)$$

where the transfer function is given by $\varphi^*(\lambda) = \alpha\lambda^{-1}[1 - p^*(\lambda)]$ according to (20). The Laplace transform of the trapping time distribution (59) is given by

$$p^*(\lambda) = 1 - (\lambda\tau_c)^\beta \Gamma(1 - \beta, \lambda\tau_c). \qquad (62)$$

Figure 7 shows the temporal evolution of the flux at a given observation point (the breakthrough curve) for different exponent β, Figure 8 for different trapping rates α. Numerical simulations coincide with the numerical inverse Laplace transform of the analytical solution (61). As shown in the figure, after an initial Fickian-like regime, a tailing regime develops where the concentration decreases as $t^{-1-\beta}$ with the exponent β given by the power law distribution of the trapping time distribution (59). For given values of τ_c and β, the occurrence of the power law regime is proportional to the trapping rate: a higher value of the trapping rate corresponds to an earlier start of the power law regime.

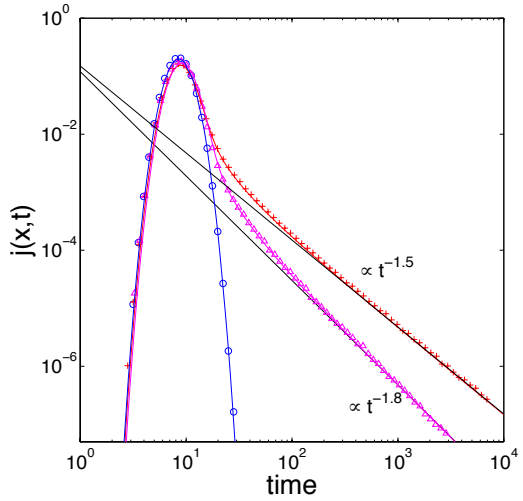

Figure 7. Temporal evolution of the flux observed at $x = 20$ with $D = 1$, $v = 2$ computed using the TDRW-MRMT solver (symbols) compared with analytical solutions (colored lines, (61)). The concentration curve without trapping (blue circles: TDRW simulation, blue line: analytical solution) is given for comparison. The characteristic time of the power low distribution of trapping time,(59), is $\tau_c = 0.1$, trapping rate: $\alpha = 0.1$ with $\beta = 0.5$ (crosses) and $\beta = 0.8$ (triangles). All values are expressed in consistent arbitrary length and time units.

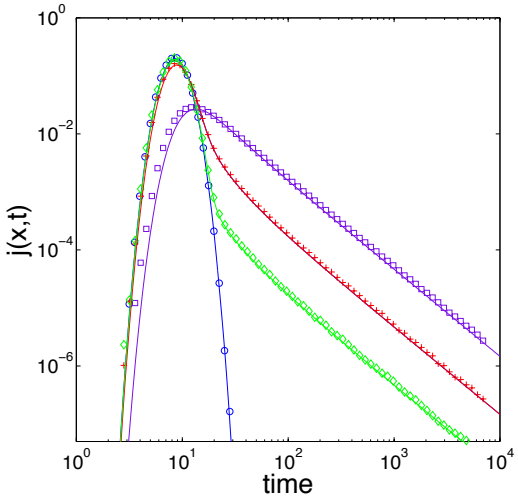

Figure 8. Temporal evolution of the flux observed at $x = 20$ with $D = 1$, $v = 2$ computed using the TDRW-MRMT solver (symbols) compared with analytical solutions (colored lines, (61)). The concentration curve without trapping (blue circles: TDRW simulation, blue line: analytical solution) is given for comparison. The characteristic time of the power low distribution of trapping time,(59), is $\tau_c = 0.1$, trapping rate: $\alpha = 1$ (squares) , $\alpha = 0.1$ (crosses) and $\alpha = 0.01$ (rhombus) for $\beta = 0.5$. All values are expressed in consistent arbitrary length and time units.

5. Conclusions

We derived a general formulation of the TDRW in heterogeneous media and described the numerical scheme for modeling the hydrodynamic transport of inert solutes in complex geometries with spatially distributed material properties and fluid velocities. We demonstrate that this TDRW scheme (7) is formally equivalent to the discretized advection-dispersion equation (1) using the equivalence to the general CTRW approach.

Then we extend the TDRW algorithm to account for mobile-immobile multirate mass transfer (TDRW-MRMT). The occurrence of trapping events in immobile zones is taken into account by incrementing the transition times by random trapping times according to a compound Poisson process. The occurrence of trapping events at a given site is described by the trapping rate, which is a property of the medium and can be spatially distributed. The multirate mass transfer extension can give rise to long tailing behavior of the BTC curves which is controlled by the trapping rate and the distribution of trapping times.

In the second part of this paper we describe the implementation of the TDRW scheme with particular attention to the robust modeling of different boundaries and initial conditions. Considering that the TDRW is based on a lattice random walk, the numerical scheme induces numerical dispersion. We derived an explicit expression for the numerical dispersion effect, which yields a Peclet criterion for the spatial discretization.

We verified that the proposed TDRW approach is a computationally efficient method to model transport problems even in heterogeneous and complex geometries because of its intrinsic compliance with parallel computing due to the independence of particle displacements. Furthermore, the system matrix of transition probability and transition time has to be calculated only once and then is stored in memory. Accordingly the only limiting factor in terms of problem size is the size of the shared memory. For example *Gjetvaj et al.* [2015] solved recently the transport of an inert solute in the porosity of a 10^6 cells discretized sample of Berea sandstone (i.e. about 10^8 computation nodes) using a 12-cores Intel Xeon (2.6 GHz) computer with 24 GB RAM using 10^6 particles. The computations were done in few tens of minutes depending on the value of the Peclet number.

Furthermore we demonstrated the accuracy of the numerical implementation of the proposed TDRW and TDRW-MRMT algorithm comparing the TDRW results with a set of analytical solutions for different configurations of homogeneous and inhomogeneous flow conditions and different initial and boundary conditions. In conclusion, TDRW provides a robust and efficient numerical method for the solution of hydrodynamic transport in heterogeneous media under multirate mass transfer.

References

Abramowitz, M., and I. A. Stegun, *Handbook of Mathematical Functions*, Dover Publications, New York, 1972.

Banton, O., F. Delay, and G. Porel, A new time domain random walk method for solute transport in 1-D heterogeneous media, *Ground Water*, *35*, 1008–1013, 1997.

Bear, J., *Dynamics of fluids in porous media*, American Elsevier, New York, 1972.

Benson, D. A., and M. M. Meerschaert, A simple and efficient random walk solution of multi-rate mobile/immobile mass transport equations, *Adv. Water Resour.*, *32*, 532–539, 2009.

Berkowitz, B., and H. Scher, Anomalous transport in random fracture networks, *Phys. Rev. Lett.*, *79*(20), 4038–4041, 1997.

Berkowitz, B., J. Klafter, R. Metzler, and H. Scher, Physical pictures of transport in heterogeneous media: Advection-dispersion, random-walk, and fractional derivative formulations, *Water Resour. Res.*, *38*(10), 1191, doi: 10.1029/2001WR001030, 2002.

Berkowitz, B., A. Cortis, M. Dentz, and H. Scher, Modeling non-fickian transport in geological formations as a continuous time random walk, *Rev. Geophys.*, *44*, RG2003, 2006.

Bodin, J., From analytical solutions of solute transport equations to multidimensional time-domain random walk (TDRW) algorithms, *Water Resources Research*, *51*, 1860–1871, doi: 10.1002/2014WR016259, 2015.

Bolster, D., M. Dentz, and T. Le Borgne, Hyper mixing in shear flow, *Water Resour. Res.*, *47*, W09,602, 2011.

Carrera, J., X. Sanchez-Vila, I. Benet, A. Medina, G. Galarza, and J. Guimera, On matrix diffusion, formulations, solutions methods and qualitative effects, *Hydrogeol. J.*, *6(1)*, 178–190, 1998.

Cvetkovic, V., A. Fiori, and G. Dagan, Solute transport in aquifers of arbitrary variability: A time-domain random walk formulation, *Water Resources Research*, *50*(7), 5759–5773, doi:10.1002/2014WR015449, 2014.

De Anna, P., T. Le Borgne, M. Dentz, A. Tartakovsky, D. Bolster, and P. Davy, Flow intermittency, dispersion, and correlated continuous time random walks in porous media., *Phys. Rev. Lett.*, *110*(18), 184,502, 2013.

Delay, F., and J. Bodin, Time domain random walk method to simulate transport by advection-diffusion and matrix diffusion in fracture networks, *Geophys. Res. Lett.*, *28*, 4051–4054, 2001.

Delay, F., G. Porel, and P. Sardini, Modelling diffusion in a heterogeneous rock matrix with a time-domain Lagrangian method and an inversion procedure, *C. R. Geoscience*, *334*, 967–973, 2002.

Dentz, M., and B. Berkowitz, Transport behavior of a passive solute in continuous time random walks and multirate mass transfer, *Water Resour. Res.*, *39(5)*, 1111, 2003.

Dentz, M., and A. Castro, Effective transport dynamics in porous media with heterogeneous retardation properties, *Geophys. Res. Lett.*, *36*, L03,403, 2009.

Dentz, M., P. Gouze, A. Russian, J. Dweik, and F. Delay, Diffusion and trapping in heterogeneous media: An inhomogeneous continuous time random walk approach, *Adv. Water Resour.*, *49*, 13–22, 2012.

Edery, Y., A. Guadagnini, H. Scher, and B. Berkowitz, Origins of anomalous transport in heterogeneous media: Structural and dynamic controls, *Water Resour. Res.*, *50*, doi:10.1002/2013WR015,111, doi: doi:10.1002/2013WR015111, 2014.

Gjetvaj, F., A. Russian, P. Gouze, and M. Dentz, Dual control of flow field heterogeneity and immobile porosity on non-fickian transport in berea sandstone, *Water Resour. Res.*, *51*, 8273–8293, 2015.

Gouze, P., Z. Melean, T. Le Borgne, M. Dentz, and J. Carrera, Non-fickian dispersion in porous media explained by heterogeneous microscale matrix diffusion, *Water Resour. Res.*, *44*, W11,416, 2008.

Haggerty, R., and S. M. Gorelick, Multiple-rate mass transfer for modeling diffusion and surface reactions in media with pore-scale heterogeneity, *Water Resour. Res.*, *31(10)*, 2383– 2400, 1995.

James, S. C., and C. V. Chrysikolpoulos, An efficient particle tracking equation with a specified spatial step for the solution of the diffusion equation, *Chem. Eng. Sci.*, *56*, 6535–6543, 2001.

Kenkre, V. M., E. W. Montroll, and M. F. Shlesinger, Generalized master equations for continuous-time random walks, *J. Stat. Phys.*, *9*(1), 45–50, 1973.

Kinzelbach, W., The random walk method in pollutant transport simulation, in *Advances in analytical and numerical groundwater flow and quality modelling*, *C*, vol. 224, edited by E. Custodio, p. 227–246, NATO ASI, 1987.

Kreft, A., and A. Zuber, On the physical meaning of the dispersion equation and its solutions for different initial and boundary conditions, *Chem. Eng. Sci.*, *33*, 1471–1480, 1978.

Le Borgne, T., M. Dentz, and J. Carrera, A Lagrangian statistical model for transport in highly heterogeneous velocity fields, *Phys. Rev. Lett.*, *101*, 090,601, 2008.

Margolin, G., M. Dentz, and B. Berkowitz, Continuous time random walk and multirate mass transfer modeling of sorption, *Chem. Phys.*, *295*, 71–80, 2003.

McCarthy, J. F., Continuous-time random walks on random media, *J. Phys. A: Math. Gen.*, *26*, 2495–2503, 1993.

Metzler, R., and J. Klafter, The random walk's guide to anomalous diffusion: a fractional dynamics approach, *Phys. Rep.*, *339*(1), 1–77, 2000.

Neuman, S. P., and D. M. Tartakovsky, Perspective on theories of anomalous transport in heterogeneous media, *Adv. Water Resour.*, *32*, 670–680, 2009.

Noetinger, B., and T. Estebenet, Up-scaling of double porosity fractured media using continuous-time random walks methods, *Transp. Porous Media*, *39*, 315–337, 2000.

Pollock, D. W., Semianalytical computation of path lines for finite-difference models, *Ground Water*, *26*(6), 743–750, 1988.

Reimus, P. W., and S. C. James, Determining the random time step in a constant spatial step particle tracking algorithm, *Chem. Eng. Sci.*, *57*, 4429–4434, 2002.

Salamon, P., D. Fernandez-Garcia, and J. J. Gomez-Hernndez, A review and numerical assessment of the random walk particle tracking method, *Journal of Contaminant Hydrology*, *87*(3564), 277 – 305, doi: http://dx.doi.org/10.1016/j.jconhyd.2006.05.005, 2006.

Scher, H., and M. Lax, Stochastic transport in a disordered solid. I. Theory, *Phys. Rev. B*, *7*(1), 4491–4502, 1973.

Corresponding author: Anna Russian, Géoscience, Université de Montpellier 2, CNRS, Montpellier, France. (anna.russian@yahoo.it)

Marco Dentz, Institute of Environmental Assessment and Water Research (IDAEA), Spanish National Research Council (CSIC), Barcelona, Spain.

Philippe Gouze, Géoscience, Université de Montpellier 2, CNRS, Montpellier, France. (anna.russian@yahoo.it)